

The geometrowave potential quantified and unified properties in general chemistry

Z. R. Tian, Department of Chemistry/Biochemistry, and Institute for Nanoscience/Engineering, Univ. of Arkansas, Fayetteville, AR 72701, USA, rtian@uark.edu.

In the thermodynamics- and quantum mechanics (QM)-pillared general chemistry, many size-dependent properties of particles e.g. atoms, ions, molecules, clusters, and nanoparticles (NPs) haven't been quantitatively predicted and unified to date. This work has introduced a geometrowave to quantitatively predict and consistently unify these particles' geometry-quantized properties to complement the thermodynamics and QM. The properties include self-assembled NPs' inter-bonding strength, NPs self-assembly spontaneity, ions' acidity and/or basicity, reactivity of particles of all charges and geometries, macromolecules' folding and unfolding, and defects of all sizes and shapes at different surface-sites.

If predicting a spontaneous self-assembly from 64 of 2-nm Au-NPs to an 8-nm NP, either directly (*Route-A*) or stepwise (*Routes B + C*) (**Fig. 1a**), each route's Gibbs free energy change¹ $\Delta G < 0$, per the ΔG 's definition. In thermodynamics, however, the NPs' formation enthalpy (ΔH_f), entropy (ΔS_f), and ΔG_f ($\approx \Delta H_f - T\Delta S_f$) are unquantified, leaving the self-assemblies²⁻⁷

chemistry unquantifiable, incomparable, and unpredictable.

To tackle this thermodynamics problem, let's quantize the zero-dimensional (0D), 1D-, 2D-, and 3D-particles' Surface Area-to-Volume (SA/V) ratio (see the **Extended Data Table S1**) into a geometrowavenumber ($\tilde{\nu}_{GW}$) in the same unit of (length⁻¹). Thus, at $T = 298.15$ (°K) and 1 (atm), the $\tilde{\nu}_{GW}$ -based GW-potential $\mu_f^o_{GW} =$

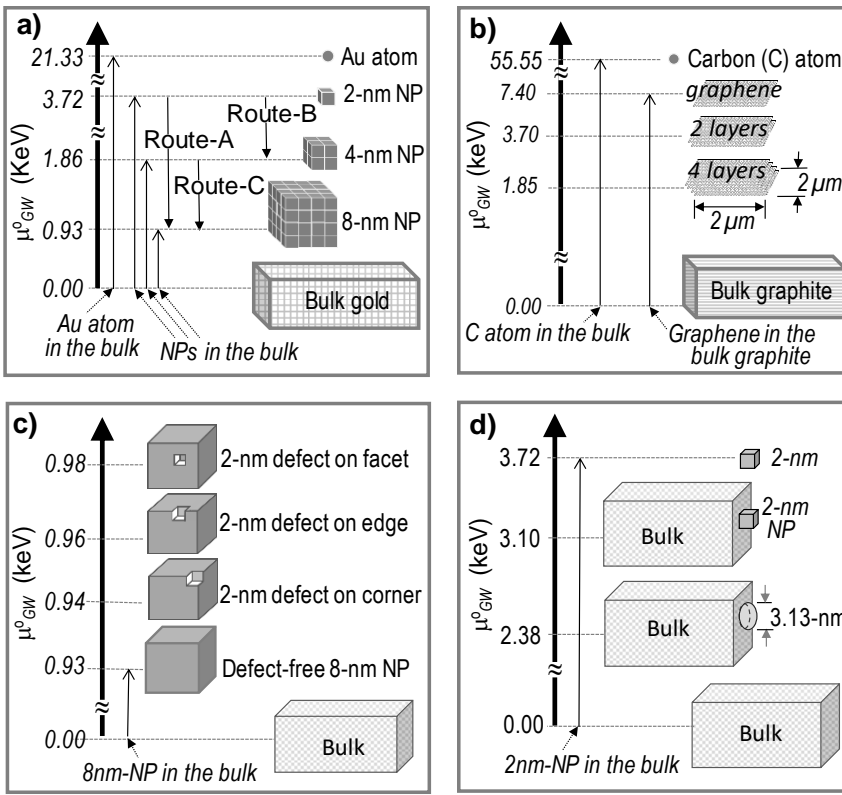


Fig. 1. The $\mu_f^0_{GW}$ values. For the Au-NPs self-assembly (a), the graphene-layers (b), a 2-nm surface-defects on an 8-nm NP (c), and a 2-nm NP's adsorption and sintering on a large surface (d).

$hc \cdot \tilde{\nu}_{GW}$, where the $c =$ speed of light, $h =$

Planck constant, and $hc \approx 1.24$ (keV·nm).

Accordingly, the

$$\bullet \Delta\mu_f^0_{GW}(\text{Route-A}) = \mu_f^0_{GW}(8\text{-nm-NP}) - 64\mu_f^0_{GW}(2\text{-nm-NPs}) = \{6/8 - 64(6/2)\}\hbar c = -237.2 \text{ (keV)},$$

$$\bullet \Delta\mu_f^0_{GW}(\text{Route-B}) = 8\mu_f^0_{GW}(4\text{-nm-NPs}) - 64\mu_f^0_{GW}(2\text{-nm-NPs}) = \{8(6/4) - 64(6/2)\}\hbar c = -223.2 \text{ (keV)},$$

$$\bullet \Delta\mu_f^0_{GW}(\text{Route-C}) = \mu_f^0_{GW}(8\text{-nm-NP}) - 8\mu_f^0_{GW}(4\text{-nm-NPs})$$

$$= \{6/8 - 8(6/4)\}\hbar c = -14.0 \text{ (keV)},$$

$$\bullet \Delta\mu_f^0_{GW}(\text{Route-A}) = \Delta\mu_f^0_{GW}(\text{Route-B}) + \Delta\mu_f^0_{GW}(\text{Route-C}),$$

which proved that the $\Delta\mu_f^0_{GW}$ is a state function.

Therefore, every NP's $\mu_f^0_{GW}$ reduction in the hierarchical self-assembly bonding (see the **Extended Data Table S2a**) is likewise quantifiable:

$$\bullet \Delta\mu_f^0_{GW}(2\text{-nm-NP in } 8\text{-nm-NP}) = \Delta\mu_f^0_{GW}(\text{Route-A})/64 = -$$

$$3.71 \text{ (keV)} = -(99.73\% \cdot \mu_f^0_{GW}(2\text{-nm-NP})),$$

$$\bullet \Delta\mu_f^0_{GW(2nm-NP \text{ in } 4nm-NP)} = \Delta\mu_f^0_{GW(\text{Route-B})}/64 = -3.49 \text{ (keV)} = -(96.16\% \cdot \mu_f^0_{GW(2nm-NP)}),$$

$$\bullet \Delta\mu_f^0_{GW(4nm-NP \text{ in } 8nm-NP)} = \Delta\mu_f^0_{GW(\text{Route-C})}/8 = -1.75 \text{ (keV)} = -(94.09\% \cdot \mu_f^0_{GW(4nm-NP)}).$$

These have concluded the larger NPs' inter-bonding weaker than smaller NPs', depending on NPs' geometry and regardless NPs' chemical composition, and every NP's $\mu_f^0_{GW}$ -decrease near 100% in the bulk since $\tilde{\nu}_{GW(bulk)}^0 = 0$ i.e. $\mu_f^0_{GW(bulk)} = 0$. This hierarchical bonding, driven by minimizing smaller particles higher $\mu_f^0_{GW}$ which is generalizable to all-scales' self-assemblies²⁻⁷, can help expand the Chemical Bonding Theory⁸.

Assuming $\Delta H_f^0_{GW} \ll \Delta\mu_f^0_{GW}$, then $\Delta S_f^0_{GW(environment)} = -\Delta H_f^0_{GW}/T \approx 0$, and $\Delta S_f^0_{GW} \approx -\Delta\mu_f^0_{GW}/T > 0$. This can help quantitatively predict the $S_f^0_{GW}$ and $\mu_f^0_{GW}$ (see the **Extended Data Table S1**) to expand the Boltzmann entropy-supported thermodynamics. For a mole of 8-nm NPs at $T = 298$ (°K),

$$\bullet \mu_{mf}^0_{GW(8nm-AuNP)} = 0.93 \text{ (keV/NP)} \times (6.023 \times 10^{23}) \text{ (NP/mole)} \times (1.60 \times 10^{-19}) \text{ (kJ/keV)} \approx 8.96 \times 10^4 \text{ (kJ/mole)}, \text{ and}$$

$$\bullet S_{mf}^0_{GW(8nm-AuNP)} = -\mu_{mf}^0_{GW(8nm-AuNP)}/298 \approx -3.01 \times 10^5 \text{ (J/K·mole)}.$$

If folding a 150-nm long 1D-polyethylene (PE) to an 8-nm NP (or backward unfolding), given the $d_{(\text{ethylene})} \approx 0.390 \text{ (nm)}^9$, the

$$\bullet \Delta\mu_f^0_{GW(Folding)} = \mu_f^0_{GW(0D-PE-NP)} - \mu_f^0_{GW(1D-PE-oligomer)} \approx (6/8)hc - (4/0.390)hc = -11.78 \text{ (keV)} = -\Delta\mu_f^0_{GW(Unfolding)}.$$

This can help generalize a thinner 1D-NP's greater $\mu_f^0_{GW}$ (see the **Extended Data Table S1**) for quantifying macromolecules' chemical bonding, as exemplified in the **Extended Data Table S2a**.

Given the $\Delta\mu_f^0_{GW(bulk \text{ graphite})} = 0$ and $d_{(\text{C-atom})} \approx 0.134 \text{ (nm)}^{10}$, the $\mu_f^0_{GW}$ (see the **Extended Data Table S2b**) can help characterize large graphenes of different layers (~0.335 nm/layer) (**Fig. 1b**). The **Fig.**

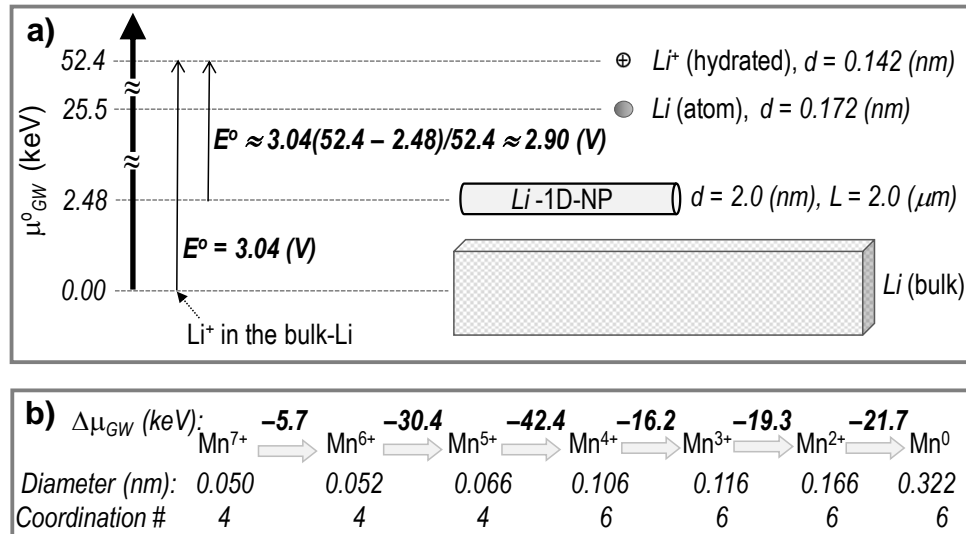


Fig. 2. The μ_{GW}^o values. Through the steps from the bulk-Li to 1D-Li-NP, Li-atom, and $\text{Li}^+(\text{aq.})$ (a), and that from Mn^{7+} to Mn^0 (b).

1b can help quantify all thinner 2D-materials' higher $\mu_{f GW}^o$ generally.

On an 8nm-NP, the $\mu_{f GW}^o$ values of 2.0 nm-sized surface defects (see the **Extended Data Table S2c**) are facet-defect's > edge-defect's > corner-defect's (**Fig. 1c**). This can help generalize all smaller defects' higher reactivity in the same order, and in turn study quantitatively the zeolites pores, proteins pockets and channels, and semiconductor defects. On a bulk flat surface, the 2.0 nm-sized NP's spontaneous adsorption and "sintering" (see the **Extended**

Data Table S2d) are each quantitatively characterizable (**Fig. 1d**). This can help quantitatively predict the $\mu_{f QGD}^o$ in the Surface Chemistry and Catalytic Chemistry, generally.

In Li-ion batteries¹¹⁻¹³, the electrochemically hard-to-measuring¹⁴ reduction potential from a $\text{Li}^+(\text{aq.})$ ¹⁵ to a 2- μm -long, 2-nm-thick Li-1D-NP electrode (**Fig. 2a**) is estimable (see the **Extended Data Table S2e**),

$$\bullet E^o(\text{cation-to-NP}) = E^o(\text{cation-to-bulk}) \cdot (\mu_{f GW(\text{cation})}^o - \mu_{f GW(\text{NP})}^o) / \mu_{f GW(\text{cation})}^o \approx -2.90 \text{ (V)}.$$

This can help quantify the $\Delta\mu_f^o_{GW}$ change (**Fig. 2b**) between NPs, atoms, and ions (see the **Extended Data Tables S2f&S3**) for expanding the electrochemistry, redox chemistry, and Lewis acid-base chemistry with ions' $\mu_f^o_{GW}$ -quantified acidity and basicity e.g. (6/d)(ion-charges).

The **Extended Data Table S1** further supports a $\mu_f^o_{GW}$ -generalized nomenclature, “ $\tilde{\nu}_{GW}$ -(point-group)-composition”, for characterizing NP-compounds. For example,

an 1.5-nm PbS-0D-NP can be thus-labeled as (6/1.5)-(R₃)-PbS, a 10-nm 0D-ZnSe-NP as (6/10)-(R₃)-ZnSe, their 1:1 compound as (6/1.5)-(R₃)-PbS•(6/10)-(R₃)-ZnSe, the 1.5-nm PbS-0D-NPs' linear 100mer as 1D-{(6/1.5)-(D_{∞d})-PbS}₁₀₀, and a 2-nm 0D-ZnO-NP's compound with kinesin as (6/3)-(R₃)-ZnO-NP•kinesin.

In conclusion, the thermodynamics- and QM-complemented $\mu_f^o_{GW}$ enables us to consistently unify and quantitatively compare and predict the particles' GW-

Table 1. Periodicities of Atoms and Monoatomic Ions $\tilde{\nu}_{GW}$ Values																		
H 0.106 56.6 2.20	Be 0.234 20.6 0.98	La 0.308 19.5 1.10	Atomic Symbol Atomic diameter* {unit: (nm)} $\tilde{\nu}_{GW}$ {unit: (nm ⁻¹)} Pauling's EN**	B 0.174 34.5 2.04	C 0.134 44.8 2.55	N 0.112 53.6 3.04	O 0.096 62.5 3.44	F 0.084 71.4 3.98	He 0.062 96.8									
Li 0.224 26.8 1.57	Na 0.380 15.8 0.93	Mg 0.290 20.7 1.31	Sc 0.368 16.3 1.36	Ti 0.352 17.0 1.54	V 0.342 17.5 1.63	Cr 0.332 18.1 1.66	Mn 0.322 18.6 1.55	Fe 0.312 19.2 1.83	Co 0.304 19.7 1.88	Ni 0.298 20.1 1.91	Cu 0.290 20.7 1.90	Zn 0.282 21.3 1.65	Al 0.236 25.4 1.61	Si 0.222 27.0 1.90	P 0.196 30.6 2.19	S 0.176 34.1 2.58	Cl 0.158 38.0 3.16	Ar 0.142 42.3
K 0.486 12.3 0.82	Ca 0.388 15.5 1.00	Sc 0.368 16.3 1.36	Ti 0.352 17.0 1.54	V 0.342 17.5 1.63	Cr 0.332 18.1 1.66	Mn 0.322 18.6 1.55	Fe 0.312 19.2 1.83	Co 0.304 19.7 1.88	Ni 0.298 20.1 1.91	Cu 0.290 20.7 1.90	Zn 0.282 21.3 1.65	Ga 0.272 22.1 1.81	Ge 0.250 24.0 2.01	As 0.228 26.3 2.18	Se 0.206 29.1 2.55	Br 0.188 31.9 2.96	Kr 0.176 34.1	
Rb 0.530 11.3 0.82	Sr 0.438 13.7 0.95	Y 0.424 14.2 1.22	Zr 0.412 14.7 1.33	Nb 0.396 15.2 1.6	Mo 0.380 15.8 2.16	Tc 0.366 16.4 2.10	Ru 0.356 16.9 2.2	Rh 0.346 17.3 2.28	Pd 0.338 17.8 2.20	Ag 0.330 18.2 1.93	Cd 0.322 18.6 1.69	In 0.312 19.2 1.78	Sn 0.290 20.7 1.96	Sb 0.266 22.6 2.05	Te 0.246 24.4 2.1	I 0.230 26.1 2.66	Xe 0.216 27.8 2.60	
Cs 0.596 10.1 0.79	Ba 0.506 11.9 0.89	La 0.390 15.4 1.10	Hf 0.416 14.4 1.3	Ta 0.400 15.0 1.5	W 0.386 15.5 1.7	Re 0.376 16.0 1.9	Os 0.370 16.2 2.2	Ir 0.360 16.7 2.2	Pt 0.354 16.9 2.4	Au 0.348 17.2 1.9	Hg 0.342 17.5 1.8	Tl 0.312 15.8 1.8	Pb 0.308 19.5 1.8	Bi 0.286 21.0 1.9	Po 0.270 22.2 2.0	At 0.300 20.0 2.2	Rn 0.240 25.0	
La 0.390 15.4 1.10	Ce 0.370 16.2 1.12	Pr 0.370 16.2 1.13	Nd 0.370 16.2 1.1	Pm 0.370 16.2 1.17	Sm 0.370 16.2 1.17	Eu 0.370 16.2 1.20	Gd 0.360 16.7 1.20	Tb 0.350 17.1 1.22	Dy 0.350 17.1 1.23	Ho 0.350 17.1 1.24	Er 0.350 17.1 1.25	Tm 0.350 17.1 1.0	Yb 0.350 17.1 1.0	Lu 0.350 17.1 1.0				
Ac 0.390 15.4 1.1	Th 0.360 16.7 1.3	Pa 0.360 16.7 1.5	U 0.350 17.1 1.7	Np 0.350 17.1 1.3	Pu 0.350 17.1 1.3	Am 0.350 25.2 1.3	Cm 0.238 25.2 1.3	Bk 0.34 17.6 1.3	Cf 0.372 16.1 1.3	Es 0.372 16.1 1.3	Fm 0.334 18.0 1.3	Md 0.346 17.3 1.3	No 0.332 18.1 1.3	Lr 0.322 18.1 1.3				

quantized properties including their hierarchical self-assembly bonding, folding–unfolding, redox activity, acidity and basicity, surface defects reactivity, etc. Atoms' and monoatomic, monovalent ions'

EN-complementary $\mu_f^o_{GW}$ (**Table 1**), generalizable to the particles and oligomers (**Extended Data Tables S1&S3**), can help develop new basics beyond the chemistry¹⁶, which should be discussed separately.

References:

- ¹ Navrotsky, A. *Physics and chemistry of earth materials* (Cambridge Univ. Press, 1994).
<https://doi.org/10.1017/CBO9781139173650>.
- ² Whitesides, G. W. and Grzybowski, B. Self-assembly at all scales. *Sci.* **295**, 2418–2421 (2002).
[10.1126/science.1070821](https://doi.org/10.1126/science.1070821).
- ³ Kresge, C. T.; Leonowicz, M. E.; Roth, W. J.; Vartuli, J. C. and Beck, J. S. Ordered mesoporous molecular sieves synthesized by a liquid-crystal template mechanism. *Nature* **359**, 710-712 (1992). <https://www.nature.com/articles/359710a0>.
- ⁴ Tian, Z. R.; Tong, W.; Wang, J. Y.; Duan, N. G.; Krishnan, V. V. and Suib, S. L. Manganese oxide mesoporous structures: mixed-valent semiconducting catalysts. *Science* **276**, 926 (1997).
<https://science.sciencemag.org/content/276/5314/926>.
- ⁵ Yang, P. D.; Zhao, D.; Margolese, D. I.; Chmelka, B. F. and Stucky, G. D. Generalized syntheses of large-pore mesoporous metal oxides with semicrystalline frameworks. *Nature* **396**, 152-155 (1998). <https://www.nature.com/articles/24132>.
- ⁶ Aizenberg, J.; Weaver, J. C.; Thanawala, M. S.; Sundar, V. C.; Morse, D. E. and Fratzl, P. Skeleton of *Euplectella* sp.: structural hierarchy from the nanoscale to the macroscale. *Science* **309**, 275-278 (2005). <https://science.sciencemag.org/content/309/5732/275>.

- ⁷ Hua, L; Zheng, J.; Zhou, Z. R.; and Tian, Z. R. Water-Switchable Interfacial Bonding on Tooth Enamel Surface, *ACS Biomater. Sci. Eng.* **4** (7), 2364–2369 (2018).
<https://pubs.acs.org/doi/abs/10.1021/acsbiomaterials.8b00403>.
- ⁸ Pauling, L. *The Nature of the Chemical Bond* (Cornell Univ. Press, Ithaca, 1960).
[https://www.academia.edu/26073847/Pauling_L._The_nature_of_the_chemical_bond_Cornell_Univ._1960_](https://www.academia.edu/26073847/Pauling_L._The_nature_of_the_chemical_bond_Cornell_Univ._1960_.).
- ⁹ Lide, D. R. *CRC Handbook of Chemistry and Physics* (CRC Press, Boca Raton, FL, 2000).
<http://diyhpl.us/~nmz787/mems/unorganized/CRC%20Handbook%20of%20Chemistry%20and%20Physics%2085th%20edition.pdf>.
- ¹⁰ Matteucci, S.; Yampolskii, Y.; Freeman, B. D. and Pinna, I. *Materials Science of Membranes for Gas and Vapor Separation* (Wiley, Chichester, 2006).
[https://books.google.com/books?id=B9reDQAAQBAJ&pg=PA34&lpg=PA34&dq=Matteucci,+S.;+Yampolskii,+Y.;+Freeman,+B.+D.+and+Pinna,+I.+Materials+Science+of+Membranes+for+Gas+and+Vapor+Separation+\(Wiley.+Chichester,+2006\).&source=bl&ots=3g0AVZH12V&sig=ACfU3U1Eh4SKpNbUmOZcMtexUDGhvEDe3A&hl=en&sa=X&ved=2ahUKEwjtiYnvsrPkAhUMWq0KHZ7TCiQQ6AEwAXoECAgQAQ#v=onepage&q=Matteucci%2C%20S.%3B%20Yampolskii%2C%20Y.%3B%20Freeman%2C%20B.%20D.%20and%20Pinna%2C%20I.%20Materials%20Science%20of%20Membranes%20for%20Gas%20and%20Vapor%20Separation%20\(Wiley%2C%20Chichester%2C%202006\).&f=false](https://books.google.com/books?id=B9reDQAAQBAJ&pg=PA34&lpg=PA34&dq=Matteucci,+S.;+Yampolskii,+Y.;+Freeman,+B.+D.+and+Pinna,+I.+Materials+Science+of+Membranes+for+Gas+and+Vapor+Separation+(Wiley.+Chichester,+2006).&source=bl&ots=3g0AVZH12V&sig=ACfU3U1Eh4SKpNbUmOZcMtexUDGhvEDe3A&hl=en&sa=X&ved=2ahUKEwjtiYnvsrPkAhUMWq0KHZ7TCiQQ6AEwAXoECAgQAQ#v=onepage&q=Matteucci%2C%20S.%3B%20Yampolskii%2C%20Y.%3B%20Freeman%2C%20B.%20D.%20and%20Pinna%2C%20I.%20Materials%20Science%20of%20Membranes%20for%20Gas%20and%20Vapor%20Separation%20(Wiley%2C%20Chichester%2C%202006).&f=false).
- ¹¹ Whittingham, S. M. Electrical energy storage and intercalation chemistry. *Science* **192** (4244), 1126–1127 (1976). <https://science.sciencemag.org/content/192/4244/1126>.

- ¹² Padhi, A.K.; Nanjundaswamy, K.S.; and Goodenough, J.B. Phospho-Olivines as Positive Electrode Materials for Rechargeable Lithium Batteries. *J. Electrochem. Soc.* **144** (4), 1188–1194 (1997). <http://jes.ecsdl.org/content/144/4/1188.full.pdf+html>.
- ¹³ Yoshino, A. 1 - Development of the Lithium-Ion Battery and Recent Technological Trends, 1-20 *Lithium-Ion Batteries: Advances and Applications* (Elsevier, 2014).
<https://www.sciencedirect.com/science/article/pii/B9780444595133000017>.
- ¹⁴ Jussila, H.; Yang, H.; Granqvist, N. and Sun, Z. Surface plasmon resonance for characterization of large-area atomic-layer graphene film. *Optica* **3** (2), 151–158 (2016).
<https://www.osapublishing.org/optica/abstract.cfm?uri=optica-3-2-151>.
- ¹⁵ Markus, Y. Ionic Radii in Aqueous Solutions, *Chem. Rev.* **88**, 1475-1498 (1988).
<https://pubs.acs.org/doi/abs/10.1021/cr00090a003>.
- ¹⁶ G. M. Whitesides, J. Deutch. Let's get practical, *Nature* **469**, 21-22 (2011). doi: [10.1038/469021a](https://doi.org/10.1038/469021a).

Acknowledgement: The author thanks Drs. H. W. Kroto, J. T. Yates, Z. L. Wang, P. Pulay, C. D. Heyes, and H. C. Tian for fruitful discussions.

EXTENDED DATA.

I. Extended Data Tables S1–S4.

The eometrowave potential quantified and unified properties in general chemistry

Z. R. Tian, Chemistry/Biochemistry, and Institute for Nanoscience/Engineering, University of Arkansas, Fayetteville, AR 72701, USA, rtian@uark.edu.

I. Extended Data Tables.

1). Extended Data Table S1.

Table S1. Simple-Shape Particles' \tilde{v}_{GW} and Point Group (Symmetry)					
	Shape	Surface-Area (SA)	Volume (V)	\tilde{v}_{GW} (= SA/V)	Point Group
0D		πd^2	$\pi d^3/6$	$(6/d)^*$	R_3
1D		$4dL + 2d^2$	$d^2 L$	$(4/d + 2/L)**$ or $(4/d)**$ if $d \ll L$	D_{2d}
		$\pi d^2/2 + \pi dL$	$\pi d^2 L/4$	$(4/d + 2/L)**$ or $(4/d)**$ if $d \ll L$	$D_{\infty d}$
2D		$\pi D^2/2 + d\pi D$	$d\pi D^2/4$	$2/d + 4/D;$ or $2/d$ if $d \ll D$	$D_{\infty d}$
		$2(aL + aL + L^2)$	aL^2	$2/d + 2/L + 2/L;$ or $2/d$ if $d \ll L$	D_{4d}
3D		$6d^2$	d^3	$(6/d)^*$	O_h
		$2 \times 3^{1/2} d^2$	$2^{1/2} d^3/3$	$3 \times 6^{1/2}/d$	O_h
		$1.732 d^2$	$0.118 d^3$	$14.678/d$	T_d

*The spherical and cubic particles share the same \tilde{v}_{GW} formula;
**The two 1D-particles share the same \tilde{v}_{GW} formula.

2). Extended Data Table S2.

Table S2. Calculations of the μ^0_{GW}

a) $\mu^0_{GW(\text{Au-atom})} = (17.2)hc = 21.33 \text{ (keV)},$
 $\mu^0_{GW(2\text{nm-AuNP})} = (6/2)hc = 3.72 \text{ (keV)},$
 $\mu^0_{GW(4\text{nm-AuNP})} = (6/4)hc = 1.86 \text{ (keV)},$
 $\mu^0_{GW(8\text{nm-AuNP})} = (6/8)hc = 0.93 \text{ (keV)}.$

b) $\mu^0_{GW(\text{C-atom})} = (44.8)hc = 55.55 \text{ (keV)},$
 $\mu^0_{GW(\text{1-layer graphene})} = hc\{2/(1 \times 0.335)\} = 7.40,$
 $\mu^0_{GW(\text{2-layer graphene})} = hc\{2/(2 \times 0.335)\} = 3.70 \text{ (keV)},$
 $\mu^0_{GW(\text{4-layer graphene})} = hc\{2/(4 \times 0.335)\} = 1.85 \text{ (keV)}.$

c) $\mu^0_{GW(\text{facet-defect})} = hc\{\text{(SA/V)}_{(2\text{-nm defect on 8-nm NP})}\} = hc\{(4 \times 2^2 + 6 \times 8^2)/(8^3 - 2^3)\} = hc\{(4 \times 2^2 + 384)/504\} = 0.98 \text{ (keV)},$
 $\mu^0_{GW(\text{edge-defect})} = hc\{(2 \times 2^2 + 384)/504\} = 0.96 \text{ (keV)},$
 $\mu^0_{GW(\text{corner-defect})} = hc\{384/504 - 17.2\} = 0.94 \text{ (keV)}.$

d) $\mu^0_{GW(\text{2nm-NP-on-large flat surface})} = hc\{(5 \times 2^2)/8\} = 3.10 \text{ (keV)},$
 $\mu^0_{GW(\text{hemisphere-on-large flat surface})} = hc\{(\pi d^2)/(\pi d^3/6)\} \approx hc(6/d) = hc(6/3.13) = 2.38 \text{ (keV)}.$

e) $\mu^0_{GW(\text{Li(I) hydrated cation})} = hc(\text{SA/V})_{\text{hydrated-Li-(I)-cation}} = hc(6/0.142) = 52.4 \text{ (keV)},$
 $\mu^0_{GW(\text{Li atom})} = hc(\text{SA/V})_{\text{Li-atom}} = hc(20.6) = 25.5 \text{ (keV)},$
 $\mu^0_{GW(\text{Li-1D-NP})} \approx hc(4/d) = hc(4/2) = 2.48 \text{ (keV)}.$

f) $\mu^0_{GW(\text{Mn(VII})} = hc(6/0.050) = 148.8 \text{ (keV)},$
 $\mu^0_{GW(\text{Mn(VI})} = hc(6/0.052) = 143.1 \text{ (keV)},$
 $\mu^0_{GW(\text{Mn(V})} = hc(6/0.066) = 112.7 \text{ (keV)},$
 $\mu^0_{GW(\text{Mn(IV})} = hc(6/0.106) = 70.3 \text{ (keV)},$
 $\mu^0_{GW(\text{Mn(III})} = hc(6/0.116) = 64.1 \text{ (keV)},$
 $\mu^0_{GW(\text{Mn(II})} = hc(6/0.166) = 44.8 \text{ (keV)},$
 $\mu^0_{GW(\text{Mn(0})} = hc(6/0.322) = 23.1 \text{ (keV)}$

3). Extended Data Table S3.

Table S3. Hydrated monoatomic ions' $\tilde{\nu}_{GW}$ values

ions	C.N.*	r (nm)	6/d (nm ⁻¹)	Basicity (nm ⁻¹)**	ions	C.N.	r (nm)	6/d (nm ⁻¹)	Acidity (nm ⁻¹)	ions	C.N.	r (nm)	6/d (nm ⁻¹)	Acidity (nm ⁻¹)
F ⁻	6	0.133	22.6	-22.6	Br ⁻⁷	4	0.025	120	840	Fe ⁺²	4	0.063	47.6	95.2
Cl ⁻	6	0.181	16.6	-16.6		6	0.039	76.9	538.3		6	0.061	49.2	58.4
Br ⁻	6	0.196	15.3	-15.3	C ⁺⁴	4	0.015	200	800		8	0.092	32.6	65.2
I ⁻	6	0.22	13.6	-13.6		6	0.016	187.5	750	Fe ⁺³	4	0.049	61.2	183.6
OH ⁻	4	0.135	22.2	-22.2	Ca ⁺²	6	0.1	30.0	60.0		6	0.055	54.5	163.5
	6	0.137	21.9	-21.9		8	0.112	26.8	53.6		8	0.078	38.5	115.5
O ⁻²	2	0.12	25.0	-50.0		10	0.123	24.4	48.8	Ga ⁺³	4	0.047	63.8	191.4
	6	0.14	21.4	-42.8		12	0.134	22.4	44.8		6	0.062	48.4	145.2
	8	0.142	21.1	-42.2	Cd ⁺²	4	0.078	38.5	77.0	Ge ⁺²	6	0.073	41.1	82.2
S ⁻²	6	0.184	16.3	-32.6		6	0.095	31.6	63.2	Ge ⁺⁴	4	0.039	76.9	307.6
Se ⁻²	6	0.198	15.2	-30.4		8	0.11	27.3	54.6		6	0.053	56.6	226.4
Te ⁻²	6	0.221	13.6	-27.2		12	0.131	22.9	45.8	Hf ⁺⁴	4	0.058	51.7	206.8
				Acidity (nm ⁻¹)***	Ce ⁺³	6	0.101	29.7	89.1		6	0.071	42.3	169.2
Ac ⁺³	6	0.112	26.8	80.4		8	0.114	26.3	78.9		8	0.083	36.1	144.4
Ag ⁺¹	4	0.1	30.0			10	0.125	24.0	72.0	Hg ⁺¹	6	0.119	25.2	25.2
	6	0.115	26.8	26.8		12	0.134	22.4	67.2	Hg ⁺²	2	0.069	43.5	87.0
	8	0.128	23.4	23.4	Ce ⁺⁴	6	0.087	34.5	138		4	0.096	31.3	62.6
Ag ⁺²	4	0.079	38.0	76.0		8	0.097	30.9	123.6		6	0.102	29.4	58.8
	6	0.094	31.9	63.8		10	0.107	28.0	112		8	0.114	26.3	52.6
Al ⁺³	4	0.039	76.9	230.7		12	0.114	26.3	105.2	I ⁺⁵	3	0.044	68.2	341
	5	0.048	62.5	187.5	Cl ⁻⁵	3	0.095	31.6	158		6	0.095	31.6	158
	6	0.054	55.6	166.8	Cl ⁻⁷	4	0.082	36.6	256.2	I ⁺⁷	4	0.042	71.4	499.8
Am ⁺³	6	0.098	30.6	918	Co ⁺²	4	0.056	53.6	107.2		6	0.053	56.6	396.2
	8	0.109	27.5	82.5		6	0.065	46.2	92.4	In ⁺³	4	0.062	48.4	145.2
Am ⁺⁴	6	0.085	35.3	141.2		8	0.09	33.3	66.6		6	0.080	37.5	112.5
	8	0.095	31.6	126.4	Co ⁺³	6	0.055	54.5	163.5	Ir ⁺³	6	0.068	44.1	132.3
As ⁺³	6	0.058	51.7	155.1	Cr ⁺²	6	0.073	41.1	82.2	Ir ⁺⁴	6	0.063	47.6	190.4
As ⁺⁵	4	0.034	88.2	441	Cr ⁺³	6	0.062	48.4	145.2	Ir ⁺⁵	6	0.057	52.6	263
	6	0.046	65.2	326	Cr ⁺⁴	4	0.041	73.2	292.8	K ⁺¹	4	0.137	21.9	21.9
Au ⁺¹	6	0.137	21.9	21.9		6	0.055	54.5	218		6	0.138	21.7	21.7
Au ⁺³	4	0.064	46.9	140.7	Cr ⁺⁶	4	0.026	115.4	692.4		8	0.151	19.9	19.9
	6	0.085	35.3	108.9		6	0.044	68.2	409.2		12	0.164	18.3	18.3
Ba ⁺²	6	0.135	22.2	44.4	Cs ⁺¹	6	0.167	18.0	18.0	La ⁺³	6	0.103	29.1	87.3
	8	0.142	21.1	42.2		8	0.174	17.2	17.2		8	0.116	25.9	77.7
	12	0.161	18.6	37.2		10	0.181	16.6	16.6		10	0.127	23.6	708
Be ⁺²	4	0.027	111.1	222.2		12	0.188	16.0	16.0		12	0.136	22.1	66.3
	6	0.045	66.7	133.4	Cu ⁺¹	2	0.046	65.2	65.2	Li ⁺¹	4	0.059	50.8	50.8
Bi ⁺³	5	0.096	31.3	93.9		4	0.06	50.0	50.0		6	0.076	39.5	39.5
	6	0.103	29.1	87.3		6	0.077	39.0	39.0		8	0.092	32.6	32.6
	8	0.117	25.6	76.8	Cu ⁺²	4	0.057	52.6	105.2	Mg ⁺²	4	0.057	52.6	105.2
Bi ⁺⁵	6	0.076	39.5	197.5		6	0.073	41.1	82.2		6	0.072	41.7	83.4
Br ⁺⁵	3	0.031	96.8	484	F ⁺⁷	6	0.008	375.0	2625		8	0.089	33.7	67.4

*C.N.: Coordination Number

**Basicity = (6/d) x (negative charges)

***Acidity = (6/d) x (positive charges)

3). Extended Data Table S3 (continued).

Table S3. Hydrated monoatomic ions' $\tilde{\nu}_{GW}$ values (continued)

ions	C.N.	r (nm)	6/d (nm ⁻¹)	Acidity (nm ⁻¹)	ions	C.N.	r (nm)	6/d (nm ⁻¹)	Acidity (nm ⁻¹)	ions	C.N.	r (nm)	6/d (nm ⁻¹)	Acidity (nm ⁻¹)
Mn ⁺²	4	0.066	45.5	91.0	Pb ⁺⁴	4	0.065	46.2	184.8	Sr ⁺²	6	0.118	25.4	50.8
	6	0.083	36.1	72.2		6	0.078	38.5	154.0		8	0.126	23.8	47.6
	8	0.096	31.3	62.6		8	0.094	31.9	127.6		10	0.136	22.1	44.2
Mn ⁺³	6	0.058	51.7	155.1	Pd ⁺²	4	0.064	46.9	93.8	Ta ⁺³	6	0.144	20.8	41.6
	4	0.039	76.9	307.6		6	0.086	34.9	69.8		6	0.072	41.7	125.1
Mn ⁺⁴	6	0.053	56.6	226.4	Pd ⁺³	6	0.076	39.5	118.5	Ta ⁺⁴	6	0.068	44.1	176.4
Mn ⁺⁵	4	0.033	90.9	454.5	Pd ⁺⁴	6	0.062	48.4	193.6	Ta ⁺⁵	6	0.064	46.9	234.5
Mn ⁺⁶	4	0.026	115.4	692.4	Pt ⁺²	4	0.06	50.0	100.0	Tc ⁺⁴	6	0.065	46.2	184.8
Mn ⁺⁷	4	0.025	120.0	840.0	Pt ⁺³	6	0.08	37.5	75.0	Ti ⁺²	6	0.086	34.9	69.8
Mo ⁺³	6	0.069	43.5	130.5	Pt ⁺⁴	6	0.063	47.6	190.4	Ti ⁺³	6	0.067	44.8	134.4
Mo ⁺⁴	6	0.065	46.2	184.8	Rb ⁺¹	6	0.152	19.7	19.7	Ti ⁺⁴	4	0.042	71.4	285.6
Mo ⁺⁵	4	0.046	65.2	326.0	8	0.161	18.6	18.6	6	0.061	49.2	196.8		
	6	0.061	49.2	246.0	10	0.166	18.1	18.1	8	0.074	40.5	162		
Mo ⁺⁶	4	0.041	73.2	439.2	12	0.172	17.4	17.4	Tl ⁺¹	6	0.15	20.0	20.2	
	6	0.059	50.8	304.8	Re ⁺⁴	6	0.063	47.6	190.4	8	0.159	18.9	18.9	
	7	0.073	41.1	246.6	Re ⁺⁵	6	0.058	51.7	258.5	12	0.17	17.6	17.6	
N ⁺³	6	0.016	187.5	562.5	Re ⁺⁶	6	0.055	54.5	327.0	Tl ⁺³	4	0.075	40.0	120
N ⁺⁵	6	0.013	230.8	1154.0	Re ⁺⁷	4	0.038	78.9	552.3	6	0.089	33.7	101.1	
Na ⁺¹	4	0.099	30.3	30.3	6	0.053	56.6	396.2	8	0.098	30.6	91.8		
	6	0.102	29.4	29.4	Rh ⁺³	6	0.067	44.8	134.4	V ⁺²	6	0.079	38.0	76.0
	8	0.118	25.4	25.4	Rh ⁺⁴	6	0.06	50.0	200.0	V ⁺³	6	0.064	46.9	140.7
	9	0.124	24.2	24.2	Rh ⁺⁵	6	0.055	54.5	272.5	V ⁺⁴	5	0.053	56.6	226.4
	12	0.13	23.1	23.1	Ru ⁺³	6	0.068	44.1	132.3	6	0.058	51.7	206.8	
Nb ⁺³	6	0.072	41.7	125.1	Ru ⁺⁴	6	0.062	48.4	193.6	8	0.072	41.7	166.8	
	8	0.079	38.0	114.0	Ru ⁺⁵	6	0.057	52.6	263.0	V ⁺⁵	4	0.042	71.4	357
Nb ⁺⁴	6	0.068	44.1	177.6	Ru ⁺⁷	4	0.038	78.9	552.3	5	0.051	58.8	294	
Nb ⁺⁵	4	0.048	62.5	312.5	Ru ⁺⁸	4	0.036	83.3	670.4	6	0.06	50.0	250	
	6	0.064	46.9	234.5	S ⁺⁴	6	0.037	81.1	324.4	W ⁺⁴	6	0.066	45.5	182
	8	0.074	40.5	202.5	S ⁺⁶	4	0.012	250.0	1500.0	W ⁺⁵	6	0.062	48.4	242
Ni ⁺²	4	0.049	61.2	122.4	6	0.029	103.4	620.4	W ⁺⁶	4	0.042	71.4	428.4	
	6	0.069	43.5	87.0	Sb ⁺³	4	0.076	39.5	118.5	5	0.051	58.8	352.8	
Ni ⁺³	6	0.056	53.6	160.8	6	0.076	39.5	118.5	6	0.06	50.0	300		
Os ⁺⁴	6	0.063	47.6	190.4	Sb ⁺⁵	6	0.060	50.0	250.0	Y ⁺³	6	0.09	33.3	99.9
Os ⁺⁵	6	0.058	51.7	258.5	Sc ⁺³	6	0.075	40.0	120.0	8	0.102	29.4	88.2	
Os ⁺⁶	6	0.055	54.5	327.0	8	0.087	34.5	103.5	9	0.108	27.8	83.4		
Os ⁺⁸	6	0.039	76.9	615.2	Se ⁺⁴	6	0.050	60.0	240.0	Zn ⁺²	4	0.06	50.0	100
P ⁺⁵	4	0.017	176.5	882.5	Se ⁺⁶	4	0.028	107.1	642.6	6	0.074	40.5	81	
	6	0.038	78.9	394.5	6	0.042	71.4	428.4	8	0.09	33.3	66.6		
Pb ⁺²	6	0.119	25.2	50.4	Si ⁺⁴	4	0.026	115.4	461.6	Zr ⁺⁴	4	0.059	50.8	203.2
	8	0.129	23.3	46.6	6	0.04	75.0	300.0	6	0.072	41.7	166.8		
	10	0.14	21.4	42.8	Sn ⁺⁴	4	0.055	54.5	218.0	8	0.084	35.7	142.8	
12	0.149	20.1	40.2	6	0.069	43.5	174.0	9	0.089	33.7	134.8			
	8	0.081	37.0	148.0										